Chinese Journal of Chemical Engineering 89 (2026) 267–276

Contents lists available at ScienceDirect

Chinese Journal of Chemical Engineering

journal homepage: www.elsevier.com/locate/CJChE

Full Length Article

Quality related fault detection based on dynamic-inner convolutional autoencoder and partial least squares and its application to ironmaking process

Ping Wu [1, 2, *], Yuxuan Ni [1], Huaimin Wang [1], Xuguang Hu [1], Zhenquan Wu [3], Jian Jiang [4], Yaowu Hu [5]

[1] *School of Information Science and Engineering, Zhejiang Sci-Tech University, Hangzhou 310018, China*
[2] *Changshan Research Institute, Zhejiang Sci-Tech University, Changshan 324299, China*
[3] *Zhejiang Sanhua Automotive Components Co., Ltd., Hangzhou 310018, China*
[4] *Zhejiang Deli Machine Manufacturer Co., Ltd., Lishui 321499, China*
[5] *Jinyun Research Institute, Zhejiang Sci-Tech University, Jinyun 321499, China*

ARTICLE INFO

Article history:
Received 20 March 2025
Received in revised form
21 August 2025
Accepted 22 August 2025
Available online 15 October 2025

Keywords:
Partial least squares
Dynamic-inner convolutional autoencoder
Quality-related fault detection
Neural networks
Safety
Dynamic modeling

ABSTRACT

Partial least squares (PLS) model maximizes the covariance between process variables and quality variables, making it widely used in quality-related fault detection. However, traditional PLS methods focus primarily on linear processes, leading to poor performance in dynamic nonlinear processes. In this paper, a novel quality-related fault detection method, named DiCAE-PLS, is developed by combining dynamic-inner convolutional autoencoder with PLS. In the proposed DiCAE-PLS method, latent features are first extracted through dynamic-inner convolutional autoencoder (DiCAE) to capture process dynamics and nonlinearity from process variables. Then, a PLS model is established to build the relationship between the extracted latent features and the final product quality. To detect quality-related faults, Hotelling's T^2 statistic is employed. The developed quality-related fault detection is applied to the widely used industrial benchmark of the Tennessee.

1. Introduction

With the continuous improvement in awareness of production safety and product quality, quality-related fault detection has garnered increasing attention in both industry and academia [1,2]. Closed-loop control is widely employed in modern industrial processes to compensate for faults, ensuring that not every fault leads to product quality deterioration. Based on their impact on product quality, faults can generally be classified into two categories: quality-related and quality-unrelated. From a cost-effectiveness perspective, immediate corrective measures may not be necessary for quality-unrelated faults, as they do not significantly affect product standards [3]. In contrast, quality-related faults directly disrupt product quality indicators, causing deviations from specifications. Such faults demand prompt corrective action to ensure consistent product performance [4]. To determine whether a fault affects product quality, researchers have extensively studied quality-related process monitoring methods [5–9]. Detecting these faults is crucial for industrial processes, as it enhances operational reliability and safety while playing a vital role in achieving high-quality production and advancing intelligent manufacturing. Over the past decades, model-based, knowledge-based, and data-driven methods have become the mainstream approaches for fault detection [10]. Although model-based fault detection methods have been successfully applied across various industrial processes. However, for large and complex industrial processes, developing accurate mathematical models is often time-consuming and labor-intensive, limiting the practicality of model-based fault detection methods [11]. Knowledge-based methods heavily rely on expert experience. As a result, they are often inefficient in handling most industrial processes. Compared to model-based and knowledge-based methods, data-driven methods achieve the fault detection

* Corresponding author. School of Information Science and Engineering, Zhejiang Sci-Tech University, Hangzhou, 310018, China.
E-mail address: pingwu@zstu.edu.cn (P. Wu).

https://doi.org/10.1016/j.cjche.2025.08.018
1004-9541/

tasks only using historical process data [12,13]. The rapid advancements in sensors, communication networks, computer technology, and data storage have significantly reduced the costs associated with data collection, processing, and storage. Consequently, data-driven fault detection demonstrates strong adaptability in fault diagnosis and fault detection for large-scale industrial processes [14−17].

As representative data-driven quality-related fault detection methods, multivariate analysis (MVA) methods like principal component analysis (PCA) [18], independent component analysis (ICA) [19], canonical correlation analysis (CCA) [20], and partial least squares (PLS) [21] have been widely adopted due to their simplicity and effectiveness. The primary goal of quality-related fault detection is to detect abnormalities related to quality. The aforementioned methods, including principal component regression [22], canonical correlation analysis [23] and partial least squares [24] have been adapted to quality-related fault detection. Among the existing methods, PLS-based approaches are especially renowned in MVA for addressing quality-related fault detection issues, with numerous successful applications reported in the literature. PLS aims to maximize the covariance between process variables and quality variables, thereby deriving quality-related subspaces and quality-independent subspaces. Standard PLS often requires many components or latent variables which contain variations orthogonal to quality variables. Zhou *et al.* [3] proposed total projection to latent structures (T-PLS) by dividing the input space into four parts instead of two parts in standard PLS. Qin and Zheng [24] developed concurrent projection to latent structures (CPLS) to decompose the input and output data spaces to five subspaces for quality-relevant and process-relevant fault monitoring. Yin *et al.* [25] proposed modified orthogonal projections to latent structures (MOPLS) method using a new structure of preprocessing-modeling-post-processing to improves the performance of quality-related fault detection.

Dynamics and nonlinearity are inherent characteristics of industrial processes. To capture process dynamics, Li *et al.* [26] extended the T-PLS model to the dynamic total PLS (T-PLS) model, which extracts the dynamic correlations between the measurement block and the quality data block for quality-relevant modeling and monitoring of multivariate dynamic processes. Yang *et al.* [27] further advanced this approach by extending CPLS to dynamic concurrent partial least squares (DCPLS) monitoring, introducing a time-lagged variable scheme for large-scale quality-related fault detection. However, both dynamic T-PLS and dynamic CPLS have limitations in that their inner models are not explicit and can be difficult to interpret. To address this issue, Dong and Qin [28] proposed the dynamic inner PLS (DiPLS) model, which extracts dynamic latent variables through an explicit dynamic model structure that aligns with the inner dynamic model. For handling nonlinearity, PLS methods have been extended to kernel PLS (KPLS) by employing kernel methods. In KPLS, process variables are mapped to high-dimensional or even infinite-dimensional spaces, and a standard PLS model is then constructed between the kernel feature process space and the quality space. Peng *et al.* [6] extended total PLS to total kernel PLS (T-KPLS) by applying kernel methods for nonlinear quality-related fault detection. Additionally, Si *et al.* [29] developed an improved KPLS method by performing general singular value decomposition (GSVD) on the loadings calculated from the kernel matrix in KPLS for enhanced quality-related fault detection.

Although KPLS has been widely used in quality-related nonlinear fault detection, it has certain limitations. The performance of KPLS-based methods heavily depends on the selection of the kernel function and its parameters. Additionally, all training samples are involved in the online monitoring stage, which can pose computational challenges when dealing with large datasets or high-dimensional data. Furthermore, kernel methods are limited to capturing only shallow features. In recent years, deep learning has achieved significant advancements in processing images, video, audio, and sequential data such as text and speech [30]. The core of deep learning is the training of deep neural networks using effective techniques such as batch normalization and dropout. Compared to kernel methods, deep neural networks are capable of extracting deeper features from data, which has led to substantial interest in their application for fault detection and fault diagnosis [31]. Typical deep learning methods, such as convolutional neural networks (CNNs), recurrent neural networks (RNNs), and autoencoders (AEs), have been successfully applied across various domains of fault detection and fault diagnosis [32]. Among these classical neural networks, the autoencoder, as an unsupervised deep learning model, excels at extracting hidden features from process data without the need for labels, making it a popular choice for fault detection [33]. For instance, Lee *et al.* [34] employed a variational autoencoder (VAE) to address nonlinear and non-normal situations in high-dimensional processes due to the violation of normality assumptions in statistical process monitoring techniques. Cheng *et al.* [35] developed a variational recurrent autoencoder-based fault detection method in probability space to handle process nonlinearity. Li *et al.* [36] introduced a distributed-ensemble stacked autoencoder (DE-SAE) model using a stacked autoencoder (SAE) to extract both local and global information for resolving complex nonlinear relationships in industrial fault detection. Yu and Zhao [37] combined a denoising autoencoder with an elastic net to address process nonlinearity and noise interference. Shen *et al.* [38] employed a variational autoencoder (VAE) model to extract nonlinear features from irregular multirate data for fault detection. Chen *et al.* [39] proposed a one-dimensional convolutional autoencoder (1D-CAE) for learning hierarchical feature representations through noise reduction of high-dimensional process signals for fault detection and diagnosis in multivariate processes. Additionally, Zhang and Qiu [40] integrated a vector autoregressive model into a one-dimensional convolutional autoencoder to develop a dynamic-inner convolutional autoencoder (DiCAE) for modeling process latent dynamics to capture both process dynamics and nonlinearity simultaneously. However, despite these advancements, AE-based methods are still unsupervised learning algorithms and thus are limited in their ability to capture quality information in quality-related fault detection.

In recent years, many data-driven methods have also been successfully applied to the field of quality-related fault detection. Guo *et al.* [41] proposed a knowledge-driven spatial-temporal graph attention neural network (K-STGAT) to address the instability issues in quality-related fault detection caused by dynamic and temporal correlations. Ma *et al.* [42] developed a relevance variable selection variational auto-encoder (RVS-VAE), which enables the selection of quality-related variables from latent features for further fault monitoring. Yang and Yan [43], aiming to overcome the limitation of insufficient extraction of quality-related information, proposed a quality relevance maximization model based on global and local structure preservation. In this model, quality indicators are incorporated into the manifold learning framework to tightly couple feature extraction with quality measures. Zhang *et al.* [44] introduced a distributed dynamic graph embedding (DDGE) network for quality-related process monitoring, which enhances local information by integrating timestamps, domain knowledge, and quality indicators. Wang *et al.* [45] proposed a novel VAE model based on knowledge sharing and correlation weighting (KSCW-VAE), which enables concurrent detection of process quality-related faults.

Motivated by the above discussions, this work proposes a novel quality-related fault detection approach by integrating DiCAE into PLS, resulting in the DiCAE-PLS model. Compared with other methods, DiCAE-PLS is capable of effectively distinguishing between process variables and quality variables, while simultaneously addressing both the dynamic and nonlinear characteristics of process data. These features make it particularly advantageous for quality-related fault detection. In the proposed DiCAE-PLS-based quality-related fault detection method, the DiCAE model is first employed to extract latent representations from process variables. With the aid of DiCAE, nonlinear and dynamic features of the process variables are effectively captured. It can effectively extract dynamic temporal features from process data and leverage the deep learning architecture to capture complex nonlinear relationships within the data, thereby enhancing the modeling capability for complex industrial processes. Subsequently, a PLS model is established to explore the relationship between process variables and quality variables, using the extracted latent representations as inputs and quality variables as outputs. The PLS model decomposes the process data space into quality-related and process-related subspaces. Finally, Hotelling's T^2 is constructed to detect quality-related faults. The main contributions of this work are as follows:

(1) To address the issues of process dynamics and nonlinearity in process data, DiCAE is naturally integrated into the PLS framework. The proposed DiCAE-PLS method effectively explores the relationship between process variables and quality variables.
(2) For quality-related fault detection, Hotelling's T^2 statistic is established based on the developed DiCAE-PLS model, with the control limits set using the kernel density estimation (KDE) method.
(3) To demonstrate the superior performance of the proposed DiCAE-PLS method, experiments are conducted on the widely used industrial Tennessee Eastman process benchmark and a real blast furnace ironmaking process (BFIP), comparing it with other relevant methods.

The remainder of this paper is organized as follows: Section 2 provides a brief review of PLS and AE. Section 3 presents a detailed description of the DiCAE-PLS based quality-related fault detection scheme. In Section 4, case studies on the widely used industrial Tennessee Eastman process (TEP) benchmark and a real blast furnace ironmaking process (BFIP), are conducted to demonstrate the superior performance of the proposed DiCAE-PLS model. Finally, Section 5 summarizes the conclusions.

2. Review of PLS and AE

2.1. PLS

Denote the input $\boldsymbol{X}\in\mathbb{R}^{N\times m}$ that consists of N samples with m process variables and the output $\boldsymbol{Y}\in\mathbb{R}^{N\times p}$ with p quality variables as follows,

$$\begin{cases}\boldsymbol{X}=[\boldsymbol{x}_1,\boldsymbol{x}_2,\cdots,\boldsymbol{x}_N]^{\mathrm{T}}\in\mathbb{R}^{N\times m}\\ \boldsymbol{Y}=[\boldsymbol{y}_1,\boldsymbol{y}_2,\cdots,\boldsymbol{y}_N]^{\mathrm{T}}\in\mathbb{R}^{N\times p}\end{cases}$$

where $\boldsymbol{x}_i$ and $\boldsymbol{y}_i (i=1,2,\cdots,N)$ are the process variables and quality variables, respectively.

The goal of PLS is to maximize the covariance of the input $\boldsymbol{X}$ and output $\boldsymbol{Y}$. PLS model decomposes $\boldsymbol{X}$ and $\boldsymbol{Y}$ as follows [46],

$$\begin{cases}\boldsymbol{X}=\sum_{i=1}^{L}\boldsymbol{t}_i\boldsymbol{p}_i+\boldsymbol{E}=\boldsymbol{T}\boldsymbol{P}^{\mathrm{T}}+\boldsymbol{E}\\ \boldsymbol{Y}=\sum_{i=1}^{L}\boldsymbol{t}_i\boldsymbol{q}_i+\boldsymbol{F}=\boldsymbol{T}\boldsymbol{Q}^{\mathrm{T}}+\boldsymbol{F}\end{cases} \tag{1}$$

where $\boldsymbol{T}\in\mathbb{R}^{N\times L}$ and $\boldsymbol{U}\in\mathbb{R}^{N\times L}$ are score matrices of $\boldsymbol{X}$ and $\boldsymbol{Y}$, respectively. $\boldsymbol{P}\in\mathbb{R}^{m\times L}$ and $\boldsymbol{Q}\in\mathbb{R}^{p\times L}$ are the loading matrices of $\boldsymbol{X}$ and $\boldsymbol{Y}$, respectively. $\boldsymbol{E}$ and $\boldsymbol{F}$ are the residual matrices. Specifically, the score vectors $\boldsymbol{t}_i$ are computed by using weight vectors $\boldsymbol{w}_i$ from deflated $\boldsymbol{X}$ data.

2.2. AE

Classical autoencoders (AEs) are composed of an encoder and a decoder. The encoder compresses the input data into a lower-dimensional representation, with the objective of preserving the essential information from the input while reducing minor noise variance. Subsequently, the decoder reconstructs the original input data from this latent representation [47].

Given the input $\boldsymbol{X}=[\boldsymbol{x}_1,\boldsymbol{x}_2,\cdots,\boldsymbol{x}_N]\in\mathbb{R}^{m\times N}$ which consists of N samples with m variables, the encoder and decoder are then represented as follows,

$$\boldsymbol{h}_i=\delta_1(\boldsymbol{W}_1\boldsymbol{x}_i+\boldsymbol{b}_1) \tag{2}$$

$$\widehat{\boldsymbol{x}}_i=\delta_2(\boldsymbol{W}_2\boldsymbol{x}_i+\boldsymbol{b}_2) \tag{3}$$

where $\boldsymbol{h}_i$ is the hidden features, δ_1 and δ_2 are the activation functions of the encoder and decoder, respectively. $\boldsymbol{W}_1$ and $\boldsymbol{W}_2$ are the weight matrices of the encoder and decoder, respectively. $\boldsymbol{b}_1$ and $\boldsymbol{b}_2$ are the biases of the encoder and decoder, respectively.

To train the autoencoder, the loss function is usually designed to minimize the errors between the original input $\boldsymbol{x}$ and the reconstruction $\widehat{\boldsymbol{x}}$ as small as possible. Then, the loss function is usually computed by mean square error (MSE) function,

$$\mathrm{Loss}_{\mathrm{AE}}=\mathrm{MSE}(\boldsymbol{X}-\widehat{\boldsymbol{X}})=\frac{1}{N}\sum_{i=1}^{N}\|\boldsymbol{x}_i-\widehat{\boldsymbol{x}}_i\|^2 \tag{4}$$

3. The Proposed Method

3.1. DiCAE-PLS model

To capture the nonlinear and dynamic features, the DiCAE developed in Ref. [40] is adopted. The DiCAE model combines CAE and vector autoregressive model. First, 1D CNN is used as encoder to extract the latent features $\boldsymbol{h}$.

$$\boldsymbol{h}=\delta_1(\mathrm{conv1}d^*(\boldsymbol{x})) \tag{5}$$

where δ_1 is the activation function, $\mathrm{conv1}d^*$ represents the 1-dimensional convolution with optimal parameters.

Denote $\boldsymbol{h}_i$ as the latent feature at time instant i, the VAR(p) of $\boldsymbol{h}$ is then derived as,

$$\begin{bmatrix}\boldsymbol{h}_t\\ \boldsymbol{h}_{t-1}\\ \cdots\\ \boldsymbol{h}_p\end{bmatrix}=\boldsymbol{A}_1\begin{bmatrix}\boldsymbol{h}_{t-1}\\ \boldsymbol{h}_{t-2}\\ \cdots\\ \boldsymbol{h}_{p-1}\end{bmatrix}+\boldsymbol{A}_2\begin{bmatrix}\boldsymbol{h}_{t-2}\\ \boldsymbol{h}_{t-3}\\ \cdots\\ \boldsymbol{h}_{p-2}\end{bmatrix}+\cdots+\boldsymbol{A}_p\begin{bmatrix}\boldsymbol{h}_{t-p}\\ \boldsymbol{h}_{t-p-1}\\ \cdots\\ \boldsymbol{h}_0\end{bmatrix}+\boldsymbol{c} \tag{6}$$

where $\boldsymbol{c}$ and $\boldsymbol{A}_i (i = 1, 2, \cdots, p)$ are learnable bias vector and coefficient matrices, respectively.

Different from traditional AE, the DiCAE model takes the reconstruction error and the dynamic loss (DL) into consideration simultaneously. The DL is defined as,

$$\mathrm{DL} = \mathrm{MSE}(\boldsymbol{h}_p, \boldsymbol{h}_y) \tag{7}$$

where $\boldsymbol{h}_y$ is calculated from $\boldsymbol{h}$ by discarding the value at the first index 0. $\boldsymbol{h}_p$ is the VAR prediction result.

Subsequently, the loss function of the DiCAE is defined as,

$$\mathrm{Loss}_{\mathrm{DiCAE}} = \mathrm{Loss}_{\mathrm{AE}} + \mathrm{DL} \tag{8}$$

ReLU is a widely used activation function which can avoid vanishing/exploding gradient issues in deep neural network architecture. However, the negative inputs may lead to inactive neurons in ReLU. In this work, the LeakyReLU is employed as activation function since it can avoid dead neutrons by introducing a small gradient for negative inputs to preserve some activity in the neurons [48]. The LeakyReLU is defined as,

$$\mathrm{LeakyReLU}(x) = \max(0, x) + \beta * \min(0, x) \tag{9}$$

where β is a coefficient to control the angle of the negative slope. The loss function of the DiCAE is optimized using the Adam optimization algorithm.

With the trained DiCAE model, the features h can be derived from the encoder. To establish the relationship between the features h and quality variables y, an PLS is constructed for fault detection. Assuming that the features $\boldsymbol{H} = [\boldsymbol{h}_1, \boldsymbol{h}_2, \cdots, \boldsymbol{h}_n] \in \mathbb{R}^{N \times n}$ are extracted from the input matrix $\boldsymbol{X}$, the PLS model is built as follows:

$$\begin{cases} \boldsymbol{H} = \boldsymbol{T}_{hy} \boldsymbol{P}_h^{\mathrm{T}} + \boldsymbol{E}_h \\ \boldsymbol{Y} = \boldsymbol{T}_{hy} \boldsymbol{Q}_y^{\mathrm{T}} + \boldsymbol{F}_y \end{cases} \tag{10}$$

where the score matrix $\boldsymbol{T}_{hy} \in \mathbb{R}^{N \times L}$ consist of N latent variables $\boldsymbol{t}_{hy}$. $\boldsymbol{P}_h \in \mathbb{R}^{m \times L}$ and $\boldsymbol{Q}_y \in \mathbb{R}^{p \times L}$ are the loading matrices of $\boldsymbol{H}$ and $\boldsymbol{Y}$, respectively. $\boldsymbol{E}_h$ and $\boldsymbol{F}_y$ are the residual matrices.

By combining the DiCAE and PLS model, the proposed DiCAE-PLS model is then represented as follows:

$$\begin{cases} f(\boldsymbol{X}) = \boldsymbol{T}_{hy} \boldsymbol{P}_h^{\mathrm{T}} + \boldsymbol{E}_h \\ \boldsymbol{Y} = \boldsymbol{T}_{hy} \boldsymbol{Q}_y^{\mathrm{T}} + \boldsymbol{F}_y \end{cases} \tag{11}$$

The latent variable $\boldsymbol{t}_{hy}$ can be represented as,

$$\boldsymbol{t}_{hy} = f(\boldsymbol{x}) \boldsymbol{R} \tag{12}$$

where $\boldsymbol{P}_H^{\mathrm{T}} \boldsymbol{R} = \boldsymbol{I}_L$.

3.2. DiCAE-PLS based quality-related fault detection

Similar to PLS-based quality-related fault detection methods, the quality variable space is decomposed into quality-related and quality-unrelated space from Eq. (11) in DiCAE-PLS model. Based on the latent variable $\boldsymbol{t}_{hy}$, the Hotelling's T^2 monitoring statistic is established for detecting the quality-related fault,

$$T^2 = \boldsymbol{t}_{hy} {\textstyle\sum}_T^{-1} \boldsymbol{t}_{hy}^{\mathrm{T}} \tag{13}$$

where $\sum_{\mathrm{T}} = \boldsymbol{T}_H^{\mathrm{T}} \boldsymbol{T}_H / (N-1)$ is the covariance of $\boldsymbol{t}_{hy}$. $\sum_T$ is calculated by using samples under normal condition.

To determine the upper control limit (UCL), kernel density estimation (KDE) method [49] is employed. KDE is a powerful nonparametric estimation technique of probability density function (PDF). The KDE method is widely used to deal with the violation of Gaussian assumption in fault detection. The PDF of the DiCAE-PLS T^2 is represented as follows,

$$P\left(T^2\right) = \frac{1}{N\mu} \sum_{j=1}^{N} k\left(\frac{T^2 - T^2(j)}{\mu}\right) \tag{14}$$

where μ is the kernel bandwidth, $T^2(j), j = 1, 2, \cdots, N$ are the samples of T^2. $k(\cdot)$ is the kernel function. The widely used Gaussian kernel is selected as the kernel function,

$$k(g) = \frac{1}{\sqrt{2\pi}} \exp\left(-\frac{g^2}{2}\right) \tag{15}$$

The selection criteria for μ, we adopted a rule based on the median absolute deviation (MAD) [50]. The specific implementation is as follows,

$$\mu = \mathrm{MAD} \times 1.5704 \times N^{1/5} \tag{16}$$

$$\mathrm{MAD} = \mathrm{median}(|x - \mathrm{median}(x)|) \tag{17}$$

where MAD represents the median absolute deviation, N denotes the sample size, and 1.5704 is a constant related to the choice of the kernel function.

Based on the estimated PDF, the UCL of the DiCAE-PLS T^2 monitoring statistic J_{T^2} can be computed at a significance level $\boldsymbol{\alpha}$:

$$P\left(T^2 < J_{T^2}\right) = \int_{-\infty}^{J_{T^2}} \frac{1}{N\mu} \sum_{j=1}^{N} K\left(\frac{T^2 - T^2(j)}{\mu}\right) \mathrm{d}T^2 = \alpha \tag{18}$$

With the established J_{T^2}, the quality-related fault is detected while $T^2 > J_{T^2}$. For data-driven fault detection, there are usually two phases, including offline modeling and online monitoring. The

The training procedure of the proposed DiCAE-PLS model is illustrated in Algorithm 1.

Algorithm 1: DiCAE-PLS training procedure

Input: Training dataset $\{X_i, y_i\}_{i=1}^{N}$ and the initialized parameters: DiCAE, VAR, PLS
Output: Trained parameters, Monitoring statistics thresholds

```
For epoch = 1, ⋯, epoch_max do
    For n = 1, ⋯, N do
    Calculate the output of DiCAE encoder h by Eq.(5);
    Flatten the output into latent features using VAR model h_y, h_p by Eq.(6);
    End
Calculate Loss_AE and DL to obtain the loss function Loss_DiCAE by Eqs. (7) and (8);
Adam is employed to optimize the DiCAE parameters until convergence;
End
By feeding h and the quality variable y into PLS, latent features are extracted by Eqs. (11) and (12);
Calculate the UCL of the DiCAE-PLS T^2 monitoring statistic J_T^2 by Eqs.(13)–(18);
```

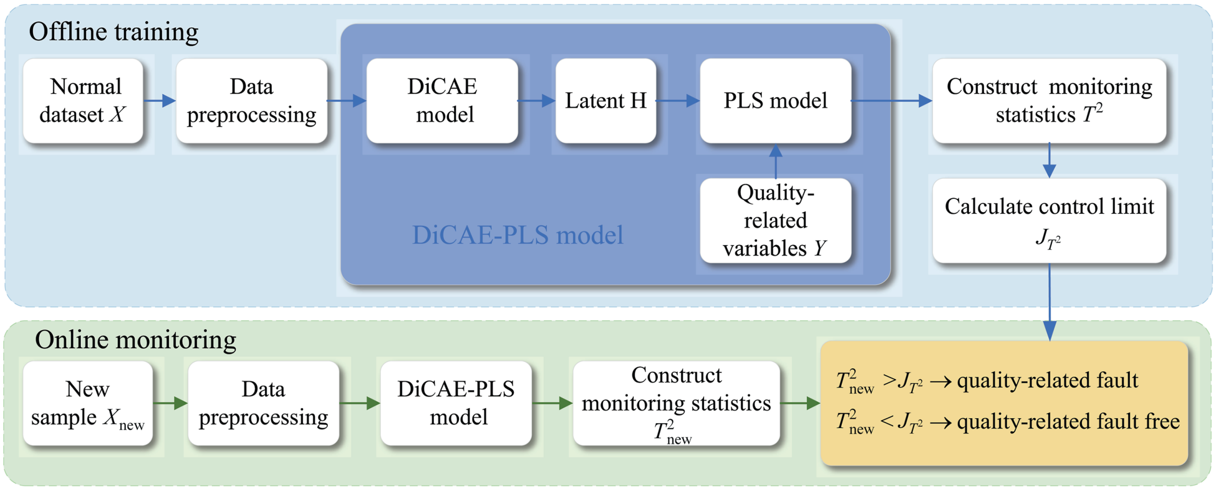

Fig. 1. Scheme of DiCAE-PLS based quality-related fault detection.

scheme of the proposed DiCAE-PLS based quality-related fault detection is depicted in Fig. 1. The details of the DiCAE-PLS-based quality-related fault detection is illustrated as follows,

- Offline training phase
  - Step 1. Normalize the collected training dataset under normal operation conditions.
  - Step 2. Build the DiCAE model to obtain the latent features h according to Eqs. (5)–(8).
  - Step 3. Establish the PLS model according to Eqs. (10)–(12).
  - Step 4. Construct monitoring statistics and determine UCL according to Eqs. (13)–(16).
- Online monitoring phase
  - Step 1. Normalize the collected new sample.
  - Step 2. Extract latent features h using the trained DiCAE.
  - Step 3. Construct the online monitoring statistic T^2 using the built DiCAE-PLS model.
  - Step 4. Compare the online monitoring statistic T^2 to the UCL J_{T^2}, and determine the quality-related faults if $T^2 > J_{T^2}$.

4. Case Studies

In this section, the proposed DiCAE-PLS method is applied to the widely used TEP benchmark and a real-world BFIP to

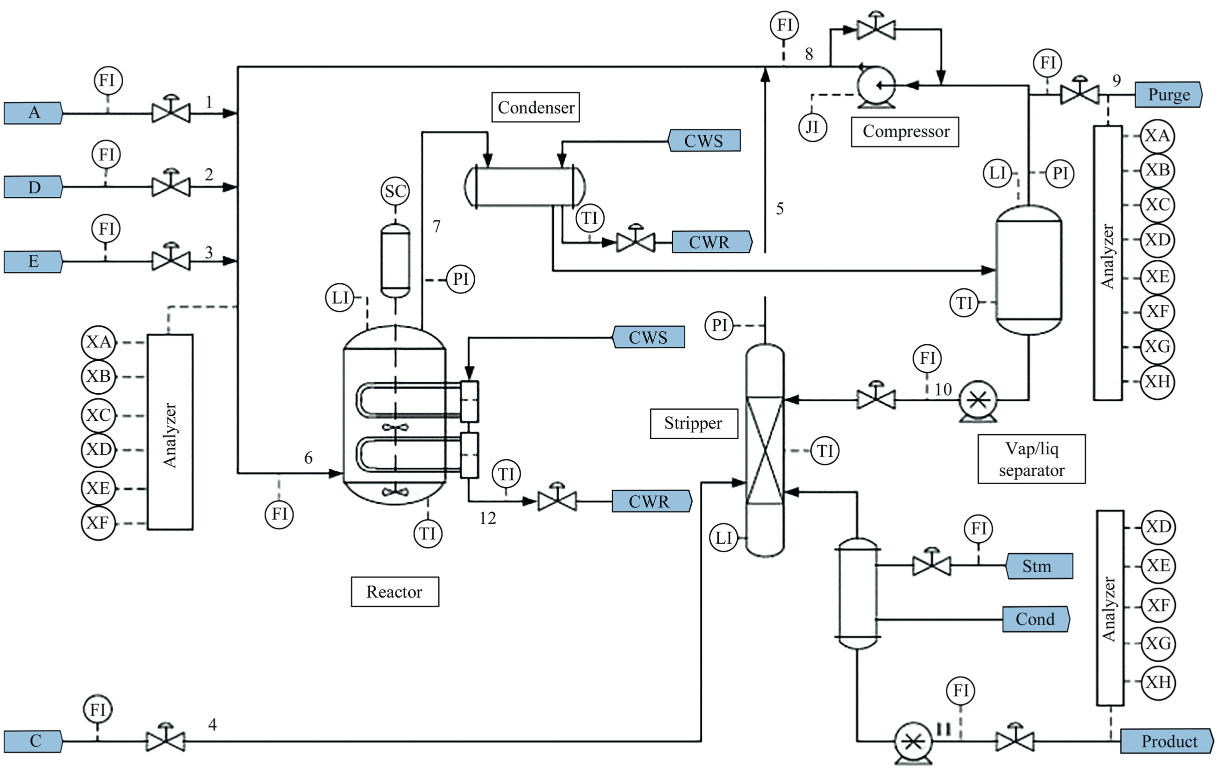

Fig. 2. Flow chart of the Tennessee Eastman process.

Table 1
Quality-related and quality-unrelated faults and their descriptions: TEP case.

	Fault	Description	Types
Quality -Related	1	A/C feed ratio, B composition constant (Stream 4)	Step
	2	B Composition A/C ratio constant (Stream 4)	Step
	5	Condenser cooling water inlet temperature	Step
	6	A feed loss (Stream 1)	Step
	7	C Header pressure loss-reduced availability	Step
	8	A, B, C feed composition (Stream 4)	Random variation
	10	C Feed temperature (Stream 4)	Random variation
	12	Condenser cooling water inlet temperature	Random variation
	13	Reaction kinetics	Slow Drift
Quality -Unrelated	3	D feed temperature (stream 2)	Step
	4	Reactor cooling water inlet temperature	Step
	9	D feed temperature (stream 2)	Random variation
	11	Reactor cooling water inlet temperature	Random variation
	15	Condenser cooling water valve	Sticking

demonstrate its capability and effectiveness. In this work, the detection of quality-related fault is our main focus. Therefore, the PLS T^2, KPLS T^2, DiPLS T^2, CAE T^2 and DiCAE T^2 are employed for comparison. To assess the quality-related fault detection quantitatively, false alarm rate (FAR) and fault detection rate (FDR) are used. FAR and FDR are defined,

$$\mathrm{FDR}=\frac{N_{\mathrm{FD}}}{N_{\mathrm{F}}}\times 100\% \tag{19}$$

$$\mathrm{FAR}=\frac{N_{\mathrm{FA}}}{N_{\mathrm{N}}}\times 100\% \tag{20}$$

where N_{F} is the total number of fault samples, N_{FD} is the number of successfully detected fault samples, N_{N} is the total number of normal samples, N_{FA} is the number of incorrectly detected normal samples.

In dynamic inner PCA (DiPCA), an inner VAR (vector autoregressive) model is applied within the PCA subspace to extract the most dynamic components—effectively maximizing the predictability of principal components (PCs) using their past values. To determine the optimal VAR order, the DiPCA model is first trained on the training dataset. The model is then applied to the validation dataset to compute the prediction error of the validation data matrix [51]. The VAR order for the proposed method is selected in a similar manner. Therefore, the VAR orders in TEP and BFIP are chosen as 1 and 1, respectively.

4.1. Tennessee Eastman process

The TEP benchmark was developed by Downs and Vogel based on a real chemical process [52]. It consists of five units: product condenser, vapor-liquid separator, reactor, recycle compressor, and product stripper. The flow chart of the TEP as shown in Fig. 2. The TEP benchmark includes 41 measurement variables (*i.e.*, XMEAS (1)-XMEAS(41)), and 12 manipulated variables (*i.e.*, XMV(1)-XMV (12)).

In this study, 33 variables (XMEAS(1)-XMEAS(22) and XMV(1)-XMV(11)) were selected as process variables, and XMEAS(38) was selected as the quality variable. There are 21 preprograming faults in TEP. Among these faults, we classified as quality-related those faults that, by altering feed composition, reaction conditions, or critical operating environments, directly or indirectly affect the quality of the output product. In addition, referring to the study by Hu *et al.* [5], we clarified the nature of faults in the TE dataset and explicitly identified Faults 1–2, 5–8, 10, and 12–13 as quality-related faults, and Faults 3, 4, 9, 11, 15 are considered to be quality-unrelated faults. Table 1 lists these faults and their detailed descriptions [52].

Table 2
FDRs and FARs of quality-related faults with different methods (%):TEP.

	Fault No.	PLS T^2	KPLS T^2	DiPLS T^2	CAE T^2	DiCAE T^2	DiCAE-PLS T^2
FDR	1	99.25	99.25	99.25	99.63	99.75	99.63
	2	97.75	97.88	98.50	97.75	97.75	98.25
	5	24.25	24.38	23.88	40.88	94.00	96.38
	6	99.25	18.63	99.13	100.00	100.00	100.00
	7	60.25	54.13	100.00	100.00	100.00	100.00
	8	94.63	96.63	97.25	95.13	96.50	97.50
	10	62.25	73.50	33.38	43.38	61.30	48.75
	12	98.25	98.88	98.38	86.13	97.50	98.88
	13	94.25	94.25	94.13	97.63	95.75	94.50
	AVERAGE	81.13	73.06	82.66	84.50	93.62	92.65
FAR	1	0	0	0	0.63	1.25	0.00
	2	0	0	1.25	0.00	0.63	0.00
	5	1.25	1.25	0.63	0.00	1.25	0.63
	6	0	0	0.63	0.63	2.50	0.63
	7	0.63	0.63	0	1.25	3.13	0.63
	8	0	0	0.63	1.88	3.13	0.00
	10	0	0	0	0.63	1.88	0.00
	12	0	0.63	0	1.25	1.88	1.25
	13	0	0	0	2.50	0.63	2.50
	AVERAGE	0.21	0.28	0.35	0.97	1.81	0.63

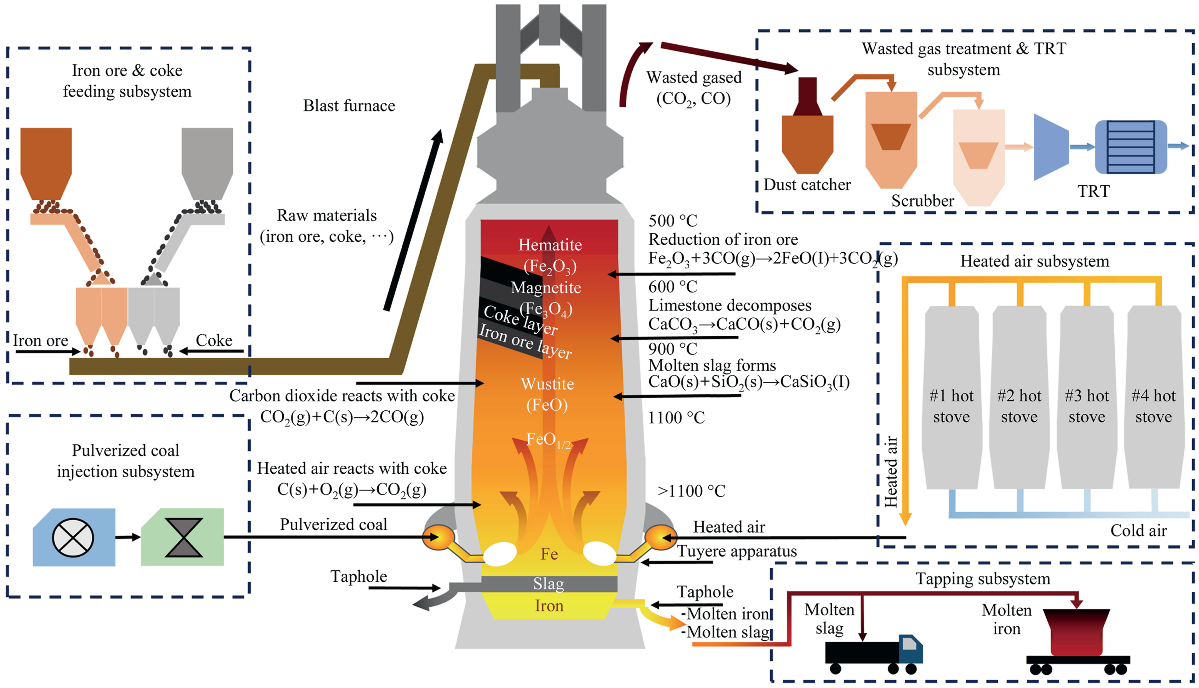

Fig. 3. The diagram of the BFIP [54].

The TEP dataset used in this study can be found in http://web.mit.edu/braatzgroup/links.html. In this dataset, 960 samples were collected under normal operating conditions as the training dataset. For a test dataset, there are also 960 samples and the fault occurred at the 161th sample. Through trial and error method, the parameters of all compared methods are set as follows. For PLS, the number of latent variables is set as 6. For KPLS, the number of latent variables is set as 7 and the kernel width is set as 5000. For DiPLS, the number of latent variables is set as 13 and the number of order is set as 50. For CAE, the model consists of two convolutional layers serving as the encoder and decoder, along with one hidden layer containing 20 nodes. And the batch size is set as 32, learning rate is set as 0.001 and kernel size is set as 3. For DiCAE, VAR is set to a first-order model. For DiCAE-PLS, the number of latent variables is set as 16. For all methods, the KDE approach is used to establish the UCL as in Ref. [49]. The confidence level α is set as 0.99 for all methods.

Table 2 presents the fault detection rates (FDRs) and false alarm rates (FARs) for quality-related faults using various methods. As indicated, the FDR of partial least squares (PLS) is 81.13%. While kernel partial least squares (KPLS) can address nonlinearity, its performance is highly dependent on the choice of kernel function and corresponding parameters. Additionally, KPLS is not effective in capturing process dynamics, leading to an average FDR of 73.06%. In contrast, by incorporating process dynamics, the DiPLS method achieves an average FDR of 82.66%. Among them, the deep learning methods CAE and DiCAE achieved higher average FDRs of 84.5% and 93.62%. However, their corresponding FARs, 0.97% and 1.81%, were higher than that of DiPLS. Among the methods evaluated, the proposed DiCAE-PLS demonstrates the best

Table 3
Measured operational and process variables of BFIP.

	No.	Description	No.	Description
Operational Variables	OV1	Oxygen-enriched rate, %	OV8	Heat wind pressure a, kPa
	OV2	Oxygen-enriched volume, 10 $km^3 \cdot h^{-1}$	OV9	Heat wind pressure b, kPa
	OV3	Cold wind volume, 10 $km^3 \cdot h^{-1}$	OV10	Outlet wind speed, $m \cdot s^{-1}$
	OV4	Top pressure a, kPa	OV11	Heat wind temperature, °C
	OV5	Top pressure b, kPa	OV12	Blower humidity, $g \cdot m^{-3}$
	OV6	Top pressure c, kPa	OV13	Coal injection setting, $t \cdot h^{-1}$
	OV7	Top pressure d, kPa		
Process Variables	PV1	Gas permeability, $m^3 \cdot min^{-1} \cdot kPa^{-1}$	PV11	Cold wind pressure b, kPa
	PV2	CO content, %	PV12	Total differential pressure, kPa
	PV3	H_2 content, %	PV13	Cold wind temperature, °C
	PV4	CO_2 content, %	PV14	Top temperature a, °C
	PV5	Blast kinetic energy, $kJ \cdot s^{-1}$	PV15	Top temperature b, °C
	PV6	Belly gas volume, $m^3 \cdot min^{-1}$	PV16	Top temperature c, °C
	PV7	Belly gas index, $m^3 \cdot (min \cdot m^2)^{-1}$	PV17	Top temperature d, °C
	PV8	Adiabatic flame temperature, °C	PV18	Drop tube temperature, °C
	PV9	Oxygen-enriched pressure, kPa	PV19	Coal injection per hour, t
	PV10	Cold wind pressure a, kPa	PV20	Coal injection in the previous hour, t

Table 4
FDRs and FARs of quality-related faults with different methods (%):BFIP.

	PLS T^2	KPLS T^2	DiPLS T^2	CAE T^2	DiCAE T^2	DiCAE-PLS T^2
FDR	93.64	96.36	92.73	90.00	99.09	99.09
FAR	2.86	4.29	4.29	11.43	15.71	2.86

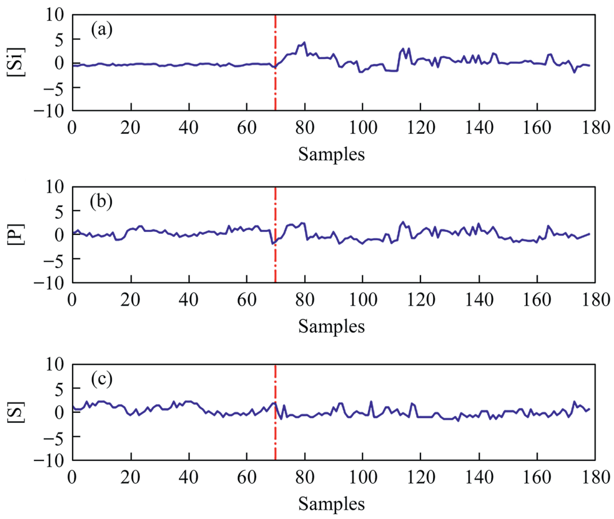

Fig. 4. The trends of normalized quality variables in BFIP test dataset.

performance, with an average FDR of 92.65%. Although the FAR of DiCAE-PLS is slightly higher than that of PLS and KPLS, its FAR of 0.63% remains lower than that of DiCAE (1.81%). These results suggest that the DiCAE-PLS method offers superior quality-related fault detection by effectively managing both nonlinearity and dynamic system behavior.

4.2. Blast furnace ironmaking process

The proposed DiCAE-PLS-based quality-related fault detection method is further applied to the blast furnace ironmaking process. Experiments are conducted on the No. 2 blast furnace at Guangxi Liuzhou Iron and Steel Company Ltd., located in Southern China. As the core unit of the ironmaking process, the blast furnace consists of five auxiliary subsystems: iron ore and coke feeding, pulverized coal injection, waste gas treatment, hot blast supply, and tapping, as illustrated in Fig. 3. In the blast furnace ironmaking process (BFIP), sintered ore, iron ore, and coke are fed into the top of the blast furnace, while pulverized coal and heated air are injected through the tuyeres at the bottom. Under high-temperature and high-pressure conditions, complex chemical and physical reactions occur within the furnace, resulting in the production of molten iron. Simultaneously, waste gases are emitted from the top of the furnace and are subsequently recycled for further use.

The blast furnace ironmaking process represents one of the most complex industrial reactor systems in metallurgical engineering. This process is frequently susceptible to abnormal operational conditions, which arise from factors such as raw material quality fluctuations, human error, and equipment malfunctions. The onset of such abnormalities can precipitate a range of adverse consequences, including elevated fuel consumption ratios, severe equipment degradation, compromised molten iron quality, and even critical safety incidents involving operational hazards and personnel risks [53]. Molten iron is a crucial product of the BFIP, playing a significant role in the efficiency and quality of subsequent steelmaking operations. Key quality indicators of molten iron include the phosphorus [P], sulfur [S], and silicon [Si] content levels, which are critical for assessing the overall quality of the iron. However, the BFIP is prone to various operational faults, such as hanging, slipping, and channeling, which can negatively impact molten iron quality. Among these, hanging has a particularly detrimental effect. Given the importance of maintaining the operational integrity of the ironmaking process, there is a critical need for quality-related fault

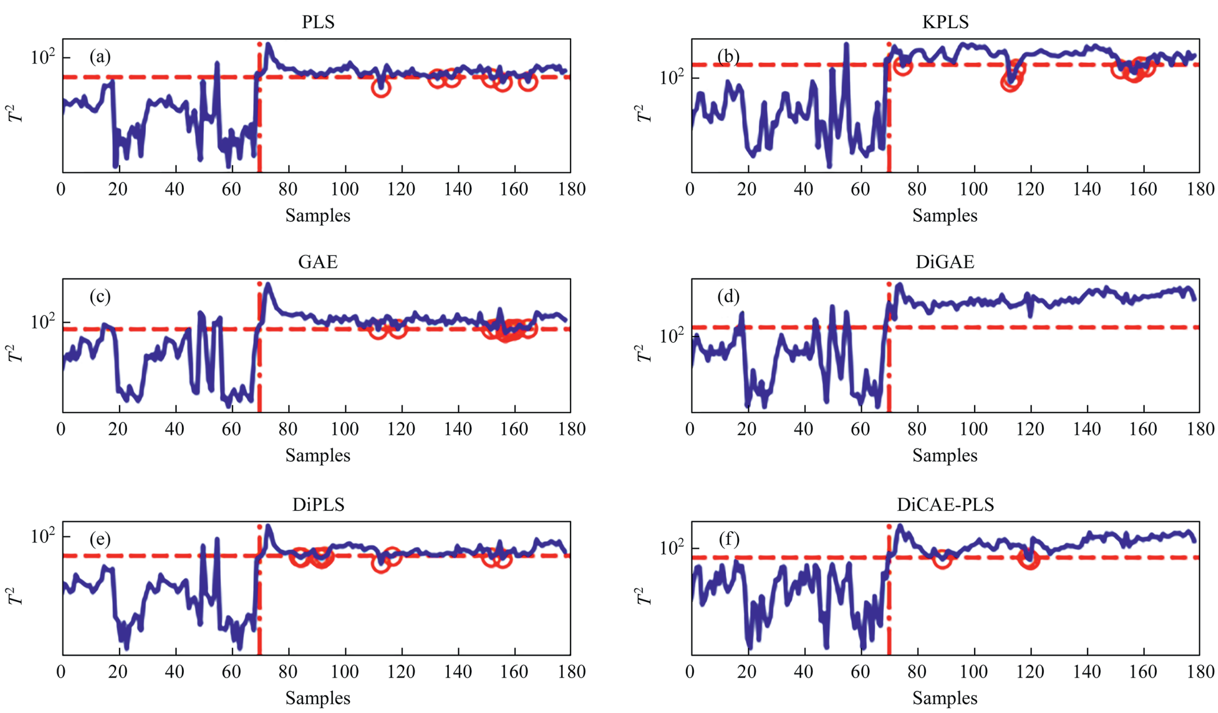

Fig. 5. The monitoring results of PLS(a), KPLS(b), CAE(c), DiCAE(d), DiPLS(e), DiCAE- PLS(f) for hanging fault: BFIP.

detection. In this study, the primary focus is on detecting the occurrence of hanging, which poses a significant challenge to maintaining the desired quality of molten iron. In this study, 3 quality variables ([Si], [P], [S]) are selected as output variables. Additionally, 13 operational variables and 20 process variables are selected as the input variables according to the expert knowledge. The operational and process variables are shown in Table 3.

In collaboration with field engineers, a total of 570 normal samples and 110 abnormal samples were collected in April 2021 according to the operation log. Out of these, 500 normal samples were designated for the training dataset, while the remaining 180 samples were allocated to the test dataset, with the fault occurring in the 71st sample. Based on experience and validation, the parameters for the comparative methods are set as follows. For PLS, the number of latent variables is set as 11. For KPLS, the number of latent variables is set as 10 and the kernel width is set as 5000. For DiPLS, the number of latent variables is set as 11 and the number of order is set as 50. For CAE, the model consists of two convolutional layers serving as the encoder and decoder, along with one hidden layer containing 20 nodes. And the batch size is set as 32, learning rate is set as 0.001 and kernel size is set as 3. For DiCAE, VAR is set to a first-order model. For DiCAE-PLS, the number of latent variables is set as 9. A confidence level of 0.99 is applied to all methods.

Table 4 presents the FDR and FAR results for various methods. As shown in Table 4, the proposed DiCAE-PLS T^2 achieves an FDR of 99.09% which is the highest among these methods. Additionally, PLS T^2, KPLS T^2, and DiPLS T^2 exhibit FDRs of 93.64%, 96.36%, and 92.73%, respectively. The FAR for these methods is relatively low, with PLS T^2 showing 2.86%, KPLS T^2 showing 4.29%, and DiPLS T^2 also showing 4.29%. Among the deep learning methods, DiCAE T^2 achieves an FDR of 99.09%, but with a relatively high FAR of 15.71%, while DiCAE-PLS T^2 achieves the same FDR of 99.09% with a FAR of 2.86%, making it the most effective in terms of both detection and false alarm rates. Overall, the proposed DiCAE-PLS T^2 exhibits superior monitoring capabilities in comparative analysis.

To further illustrate the performance of the proposed DiCAE-PLS method, Figs. 4 and 5 depict the quality variables and monitoring results of various methods, respectively. The results clearly demonstrate that the DiCAE-PLS method T^2 statistic has a low rate of missed fault alarms and a high rate of fault detection, indicating its superior monitoring capability in comparison to other methods. Experimental results from the TEP benchmark and a real blast furnace ironmaking process consistently indicate that the proposed DiCAE-PLS method demonstrates superior performance in terms of FDR and FAR, showing significant effectiveness in quality-related fault detection.

5. Conclusions

In this study, a novel quality-related fault detection method, termed DiCAE-PLS, is proposed by integrating dynamic inner convolutional autoencoders (DiCAE) with partial least squares (PLS). Specifically, features extracted from process variables using the DiCAE are utilized as inputs, while quality variables are treated as outputs. A PLS model is subsequently constructed to establish the relationship between these inputs and outputs for quality-related fault detection, with Hotelling's T^2 statistic employed as the detection criterion. The effectiveness of the proposed DiCAE-PLS method is validated through its application to the Tennessee Eastman process benchmark and a real-world blast furnace ironmaking process, demonstrating superior performance in quality-related monitoring. Despite the advantages offered by the DiCAE-PLS method, there remain areas for further enhancement. In the DiCAE-PLS framework, process variables are initially processed through the DiCAE model to extract features for subsequent analysis. To improve modeling accuracy, increasing the order of the VAR model may be beneficial, as higher-order VAR models can more effectively capture complex process dynamics. Future work may enhance generalization capability through the incorporation of regularization techniques, incremental learning, and other strategies. Moreover, it would be interesting to explore the propagation path of the process fault to the quality variable. Maybe causality analysis can be integrated in our proposed method. Additionally, further exploration of deep neural network architectures is planned to enhance feature extraction capabilities.

CRediT Authorship Contribution Statement

Ping Wu: Writing – original draft, Supervision, Methodology, Funding acquisition, Conceptualization. Yuxuan Ni: Writing – original draft, Validation, Software, Data curation. Huaimin Wang: Validation, Software, Data curation. Xuguang Hu: Writing – original draft, Software. Zhenquan Wu: Writing – review & editing. Jian Jiang: Writing – review & editing. Yaowu Hu: Writing – review & editing, Validation.

Declaration of Competing Interest

The authors declare that they have no known competing financial interests or personal relationships that could have appeared to influence the work reported in this paper.

Acknowledgements

This work was supported in part by the National Natural Science Foundation of China (62573387), the Natural Science Foundation of Zhejiang province, China (LY24F030004), the Fundamental Research Funds of Zhejiang Sci-Tech University (25222139-Y).

References

[1] Y.Q. Wang, Y.B. Si, B. Huang, Z.J. Lou, Survey on the theoretical research and engineering applications of multivariate statistics process monitoring algorithms: 2008–2017, *Can. J. Chem. Eng.* 96 (10) (2018) 2073–2085.
[2] Q. Joe, C. H, Advances and opportunities in machine learning for process data analytics, *Comput. Chem. Eng.* 126 (2019) 465–473.
[3] D.H. Zhou, G. Li, S.J. Qin, Total projection to latent structures for process monitoring, *AIChE. J.* 56 (1) (2010) 168–178.
[4] C.Y. Sun, Y.Z. Yin, H.B. Kang, H.J. Ma, A quality-related fault detection method based on the dynamic data-driven algorithm for industrial systems, *IEEE Trans. Autom. Sci. Eng.* 19 (4) (2022) 3942–3952.
[5] C.H. Hu, Z.Y. Xu, X.Y. Kong, J.Y. Luo, Recursive-CPLS-based quality-relevant and process-relevant fault monitoring with application to the Tennessee Eastman process, *IEEE Access* 7 (2019) 128746–128757.
[6] K.X. Peng, K. Zhang, G. Li, Quality-related process monitoring based on total kernel PLS model and its industrial application, *Math. Probl Eng.* 2013 (1) (2013) 707953.
[7] B. Song, H.B. Shi, S. Tan, Y. Tao, Multisubspace orthogonal canonical correlation analysis for quality-related plant-wide process monitoring, *IEEE Trans. Ind. Inform.* 17 (9) (2021) 6368–6378.
[8] K. Zhang, K.X. Peng, S.X. Ding, Z.W. Chen, X. Yang, A correlation-based distributed fault detection method and its application to a hot tandem rolling mill process, *IEEE Trans. Ind. Electron.* 67 (3) (2020) 2380–2390.
[9] B. Song, X.G. Zhou, H.B. Shi, Y. Tao, Performance-indicator-oriented concurrent subspace process monitoring method, *IEEE Trans. Ind. Electron.* 66 (7) (2018) 5535–5545.
[10] X.W. Dai, Z.W. Gao, From model, signal to knowledge: a data-driven perspective of fault detection and diagnosis, *IEEE Trans. Ind. Inform.* 9 (4) (2013) 2226–2238.
[11] Z.W. Gao, C. Cecati, S.X. Ding, A survey of fault diagnosis and fault-tolerant techniques: part I: fault diagnosis with model-based and signal-based approaches, *IEEE Trans. Ind. Electron.* 62 (6) (2015) 3757–3767.
[12] Z.Q. Ge, Z.H. Song, F.R. Gao, Review of recent research on data-based process monitoring, *Ind. Eng. Chem. Res.* 52 (10) (2013) 3543–3562.

[13] Q.C. Jiang, X.F. Yan, B. Huang, Review and perspectives of data-driven distributed monitoring for industrial plant-wide processes, *Ind. Eng. Chem. Res.* 58 (29) (2019) 12899–12912.
[14] C.H. Zhao, Perspectives on nonstationary process monitoring in the era of industrial artificial intelligence, *J. Process Control* 116 (2022) 255–272.
[15] Y.C. Jiang, S. Yin, O. Kaynak, Performance supervised plant-wide process monitoring in industry 4.0: a roadmap, *IEEE Open J. Ind. Electron. Soc.* 2 (2020) 21–35.
[16] J.S. Zeng, C. Lu, L. Yao, Y. Liu, S.H. Luo, F. Wang, C.H. Gao, Robust stacked probabilistic latent variable model for fault isolation of dynamic process with outliers, *IEEE Trans. Autom. Sci. Eng.* 21 (4) (2023) 6460–6472.
[17] L. Ma, P.P. Yang, K.X. Peng, Multitask learning based collaborative modeling of heterogeneous data for compound fault diagnosis in manufacturing processes, *IEEE Trans. Ind. Inform.* 20 (12) (2024) 14174–14183.
[18] M. Kano, S. Hasebe, I. Hashimoto, H. Ohno, A new multivariate statistical process monitoring method using principal component analysis, *Comput. Chem. Eng.* 25 (7–8) (2001) 1103–1113.
[19] J.M. Lee, C. Yoo, I.B. Lee, Statistical process monitoring with independent component analysis, *J. Process Control* 14 (5) (2004) 467–485.
[20] Z.W. Chen, S.X. Ding, K. Zhang, Z.B. Li, Z.K. Hu, Canonical correlation analysis-based fault detection methods with application to alumina evaporation process, *Control Eng. Pract.* 46 (2016) 51–58.
[21] Y.H. Qin, Z.J. Lou, Y.Q. Wang, S. Lu, P. Sun, An analytical partial least squares method for process monitoring, *Control Eng. Pract.* 124 (2022) 105182.
[22] C.Y. Sun, Y.Z. Yin, H.B. Kang, H.J. Ma, A distributed principal component regression method for quality-related fault detection and diagnosis, *Inf. Sci.* 600 (2022) 301–322.
[23] Q.Q. Zhu, Q. Liu, S.J. Qin, Concurrent quality and process monitoring with canonical correlation analysis, *J. Process Control* 60 (2017) 95–103.
[24] S.J. Qin, Y.Y. Zheng, Quality-relevant and process-relevant fault monitoring with concurrent projection to latent structures, *AIChE. J.* 59 (2) (2013) 496–504.
[25] S. Yin, G. Wang, H.J. Gao, Data-driven process monitoring based on modified orthogonal projections to latent structures, *IEEE Trans. Control Syst. Technol.* 24 (4) (2016) 1480–1487.
[26] G. Li, B.S. Liu, S.J. Qin, D.H. Zhou, Quality relevant data-driven modeling and monitoring of multivariate dynamic processes: the dynamic T-PLS approach, *IEEE Trans. Neural Netw.* 22 (12) (2011) 2262–2271.
[27] J. Yang, J.Y. Wang, J.L. Sha, H.Q. Dai, H.B. Liu, Quality-related monitoring of distributed process systems using dynamic concurrent partial least squares, *Comput. Ind. Eng.* 164 (2022) 107893.
[28] Y.N. Dong, Q. Joe, Regression on dynamic PLS structures for supervised learning of dynamic data, *J. Process Control* 68 (2018) 64–72.
[29] Y.B. Si, Y.Q. Wang, D.H. Zhou, Key-performance-indicator-related process monitoring based on improved kernel partial least squares, *IEEE Trans. Ind. Electron.* 68 (3) (2020) 2626–2636.
[30] Y. LeCun, Y. Bengio, G. Hinton, Deep learning, *Nature* 521 (7553) (2015) 436–444.
[31] R. Iqbal, T. Maniak, F. Doctor, C. Karyotis, Fault detection and isolation in industrial processes using deep learning approaches, *IEEE Trans. Ind. Inform.* 15 (5) (2019) 3077–3084.
[32] J.B. Yu, Y. Zhang, Challenges and opportunities of deep learning-based process fault detection and diagnosis: a review, *Neural Comput. Appl.* 35 (1) (2023) 211–252.
[33] J.C. Qian, Z.H. Song, Y. Yao, Z.R. Zhu, X.M. Zhang, A review on autoencoder based representation learning for fault detection and diagnosis in industrial processes, *Chemom. Intell. Lab. Syst.* 231 (2022) 104711.
[34] S. Lee, M. Kwak, K.L. Tsui, S.B. Kim, Process monitoring using variational autoencoder for high-dimensional nonlinear processes, *Eng. Appl. Artif. Intell.* 83 (2019) 13–27.
[35] F.F. Cheng, Q.P. He, J.S. Zhao, A novel process monitoring approach based on variational recurrent autoencoder, *Comput. Chem. Eng.* 129 (2019) 106515.
[36] Z.C. Li, L. Tian, Q.C. Jiang, X.F. Yan, Distributed-ensemble stacked autoencoder model for non-linear process monitoring, *Inf. Sci.* 542 (2021) 302–316.
[37] W.K. Yu, C.H. Zhao, Robust monitoring and fault isolation of nonlinear industrial processes using denoising autoencoder and elastic net, *IEEE Trans. Control Syst. Technol.* 28 (3) (2020) 1083–1091.
[38] B.B. Shen, J.C. Qian, Z.Y. Yang, L. Yao, Multirate nonlinear process fault detection based on multiscale hierarchical variational autoencoder, *IEEE Sens. J.* 24 (10) (2024) 16467–16477.
[39] S.M. Chen, J.B. Yu, S.J. Wang, One-dimensional convolutional auto-encoder-based feature learning for fault diagnosis of multivariate processes, *J. Process Control* 87 (2020) 54–67.
[40] S.Y. Zhang, T. Qiu, A dynamic-inner convolutional autoencoder for process monitoring, *Comput. Chem. Eng.* 158 (2022) 107654.
[41] L. Guo, H.B. Shi, S. Tan, B. Song, Y. Tao, A knowledge-driven spatial-temporal graph neural network for quality-related fault detection, *Process. Saf. Environ. Prot.* 184 (2024) 1512–1524.
[42] Y. Ma, H.B. Shi, S. Tan, B. Song, Y. Tao, Relevance variable selection variational auto-encoder network for quality-related nonlinear process monitoring, *Appl. Soft Comput.* 154 (2024) 111333.
[43] J.D. Yang, X.F. Yan, Global–local preserving method of quality-related maximization and its application for process monitoring, *Control Eng. Pract.* 154 (2025) 106143.
[44] W. Zhang, Y.P. Gao, J.Z. Wang, M.W. Zhao, Y.Q. Zhu, T.S. Yang, Distributed dynamic graph embedding for quality-related monitoring in the flotation process, *IEEE Trans. Instrum. Meas.* 73 (2024) 3516911.
[45] Z.Y. Wang, C.Z. Wang, Y.G. Li, Variational autoencoder based on knowledge sharing and correlation weighting for process-quality concurrent fault detection, *Eng. Appl. Artif. Intell.* 133 (2024) 108051.
[46] S. de Jong, SIMPLS: an alternative approach to partial least squares regression, *Chemom. Intell. Lab. Syst.* 18 (3) (1993) 251–263.
[47] J.H. Zhai, S.F. Zhang, J.F. Chen, Q. He, Autoencoder and its various variants. 2018 IEEE International Conference on Systems, Man, and Cybernetics (SMC). Miyazaki, Japan, IEEE, 2018, pp. 415–419.
[48] J. Xu, Z.S. Li, B.W. Du, M.M. Zhang, J. Liu, Reluplex made more practical: leaky ReLU. 2020 IEEE Symposium on Computers and Communications (ISCC), IEEE, Rennes, France, 2020, pp. 1–7.
[49] P.P. Odiowei, Y. Cao, Nonlinear dynamic process monitoring using canonical variate analysis and kernel density estimations, *IEEE Trans. Ind. Inform.* 6 (1) (2009) 36–45.
[50] A. Chaudhuri, D. Kakde, C. Sadek, L. Gonzalez, S. Kong, The mean and Median criteria for kernel bandwidth selection for support vector data description. 2017 IEEE International Conference on Data Mining Workshops (ICDMW), IEEE, New Orleans, LA, USA, 2017, pp. 842–849.
[51] Y.N. Dong, Q. Joe, A novel dynamic PCA algorithm for dynamic data modeling and process monitoring, *J. Process Control* 67 (2018) 1–11.
[52] J.J. Downs, E.F. Vogel, A plant-wide industrial process control problem, *Comput. Chem. Eng.* 17 (3) (1993) 245–255.
[53] X.Z. Zhu, D.L. Gao, C. Yang, C.J. Yang, A blast furnace fault monitoring algorithm with low false alarm rate: ensemble of greedy dynamic principal component analysis-Gaussian mixture model, *Chin. J. Chem. Eng.* 57 (2023) 151–161.
[54] S.W. Lou, C.J. Yang, X.J. Zhang, H.W. Zhang, P. Wu, Blast furnace ironmaking process monitoring with time-constrained global and local nonlinear analytic stationary subspace analysis, *IEEE Trans. Ind. Inform.* 20 (3) (2024) 3163–3176.